SUPPLEMENTARY MATERIAL

An impedimetric sensor based on molecularly imprinted nanoparticles for the determination of trypsin in artificial matrixes - towards point-of-care diagnostics

Sabrina Di Masi[1*], Marco Costa[1], Francesco Canfarotta[2*], Antonio Guerreiro[2], Alicia Hartley[2], Sergey A. Piletsky[3], Cosimino Malitesta[1]

[1]Laboratorio di Chimica Analitica, Edificio A6, DiSTeBA, Università del Salento, Via per Monteroni 73100, Lecce (Italia)

[2]MIP Discovery, Colworth Park, Sharnbrook - MK44 1LQ Bedford UK

[3] Department of Chemistry, University of Leicester, University Rd, LE1 7RH Leicester, UK

*Corresponding authors: sabrina.dimasi@unisalento.it; francesco.canfarotta@mipdiscovery.com

Content

Section 1. Sensor preparation

The Scheme **S1** shows the steps adopted for the sensor preparation.

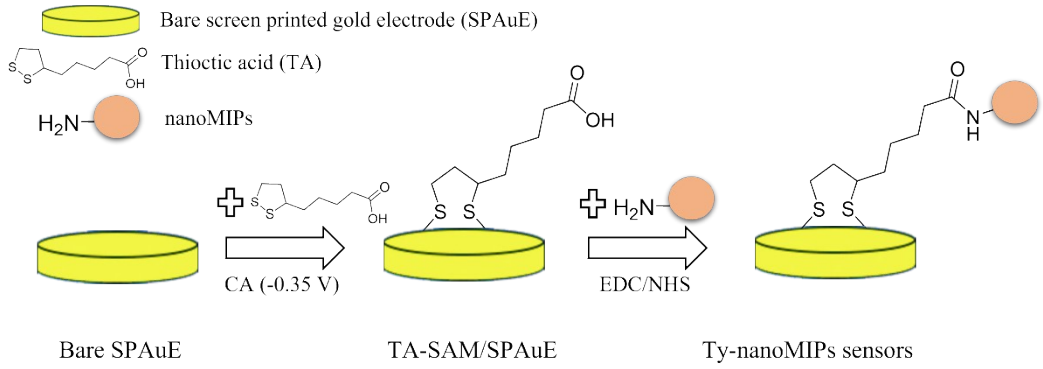

Scheme **S1**. Schematics describing the steps to immobilise nanoMIPs on sensor.

A bare SPAuE electrode was functionalised by applying a chronoamperometric measurement at -0.35 V (*vs* Ag reference) in the presence of 3 mg/mL of thioctic acid (TA) dissolved in ethanol. Afterwards, the obtained TA-SAM was activated by EDC/NHS coupling, promoting the attachment (immobilisation) of the nanoMIPs through their primary available amine groups. The same protocol was adopted for the preparation of the control (NIP sensor).

Section 2. Electrochemical impedance spectroscopy measurements

EIS data were represented by Nyquist plots and consisted of a high-frequency semicircle and straight line at low-frequency range. The circuit elements include a charge transfer resistance in series with Warburg impedance to represent the solution resistance and the diffusion part, respectively, and in parallel the constant phase element (instead of double layer capacitance) because of the non-uniform distribution of capacitance over the electrode surface. The semicircle portion reflects the electron transfer kinetics, while the straight line represents the diffusion of the redox molecules from the bulk solution to/from the electrode surface. The surface properties of modified electrodes surface were measured by means of the electron transfer resistance (R_{ct}) and compared during EIS characterisation studies, and the analytical assessment, respectively. The equivalent circuit used for the experimental data fitting was the Randle's circuit, as shown in Fig. **S1**.

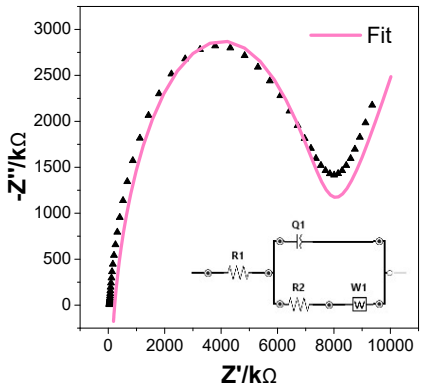

Fig. **S1**. Example of raw experimental EIS data fitted with the Randle's equivalent circuit (inset graph).

Section 3. Characterisation of nanoMIPs: Transmission Electron Microscopy (TEM) and Dynamic Light Scattering (DLS) analysis

DLS and TEM measurements on SOL-Ty-nanoMIPs and SP-Ty-nanoMIPs have been performed and shown in Fig. **S2** and **S3**, respectively.

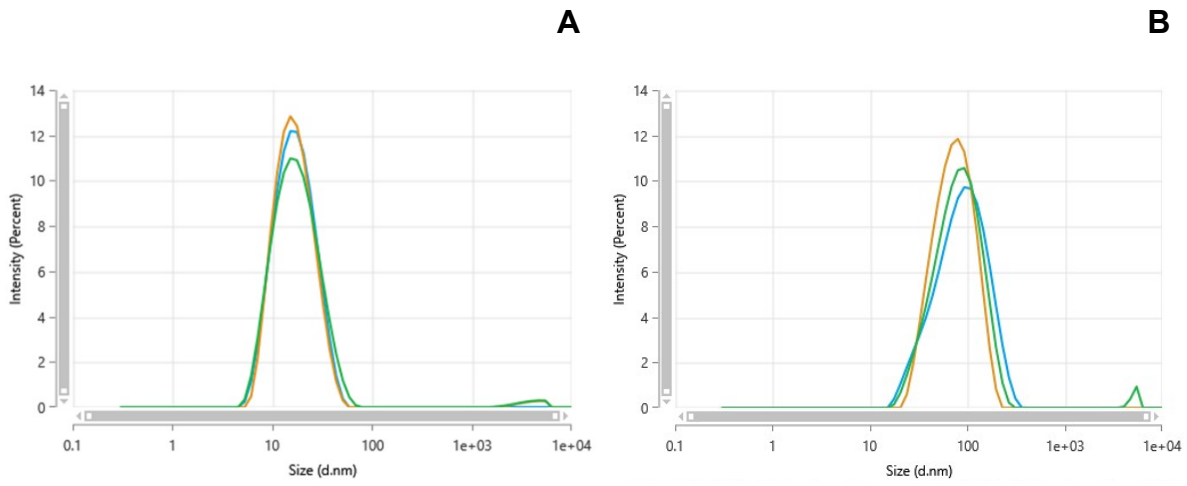

Fig. **S2.** Dynamic light scattering (DLS) measurements on (A) SOL-Ty-nanoMIPs with a Z-average of 15.3 ± 0.3 nm and (B) SP-Ty-nanoMIPs, with a Z-average of 74.1 ± 0.5 nm, respectively.

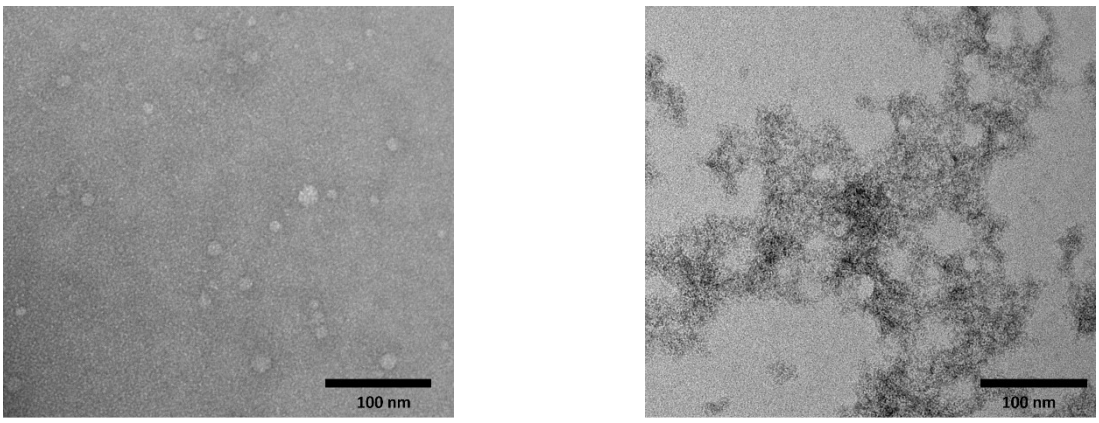

Fig. **S3.** Transmission electron microscopy (TEM) analysis on SP-Ty-nanoMIP (left) and SOL-Ty-nanoMIPs (right), respectively (x 50k magnification).

Section 4. Electrochemical characterisation of TA-SAMs

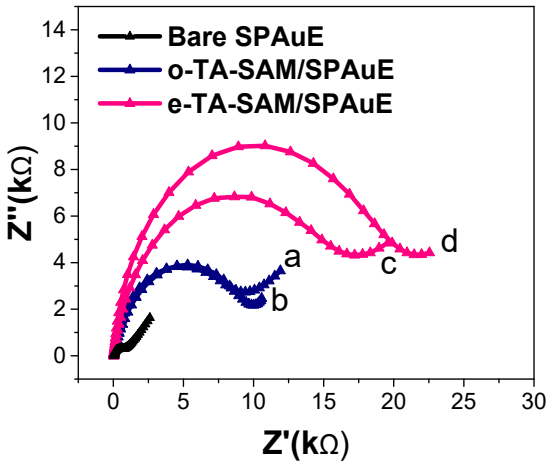

Fig. **S4.** Nyquist plots of bare SPAuE (blank line), o-TA-SAM/SPAuE (navy line), and e-TA-SAM/SPAuE (pink line), after (a,c) TA-SAM preparation, and (b,d) nanoMIPs immobilisation.

Section 5. Preliminary tests on nanoMIPs selection

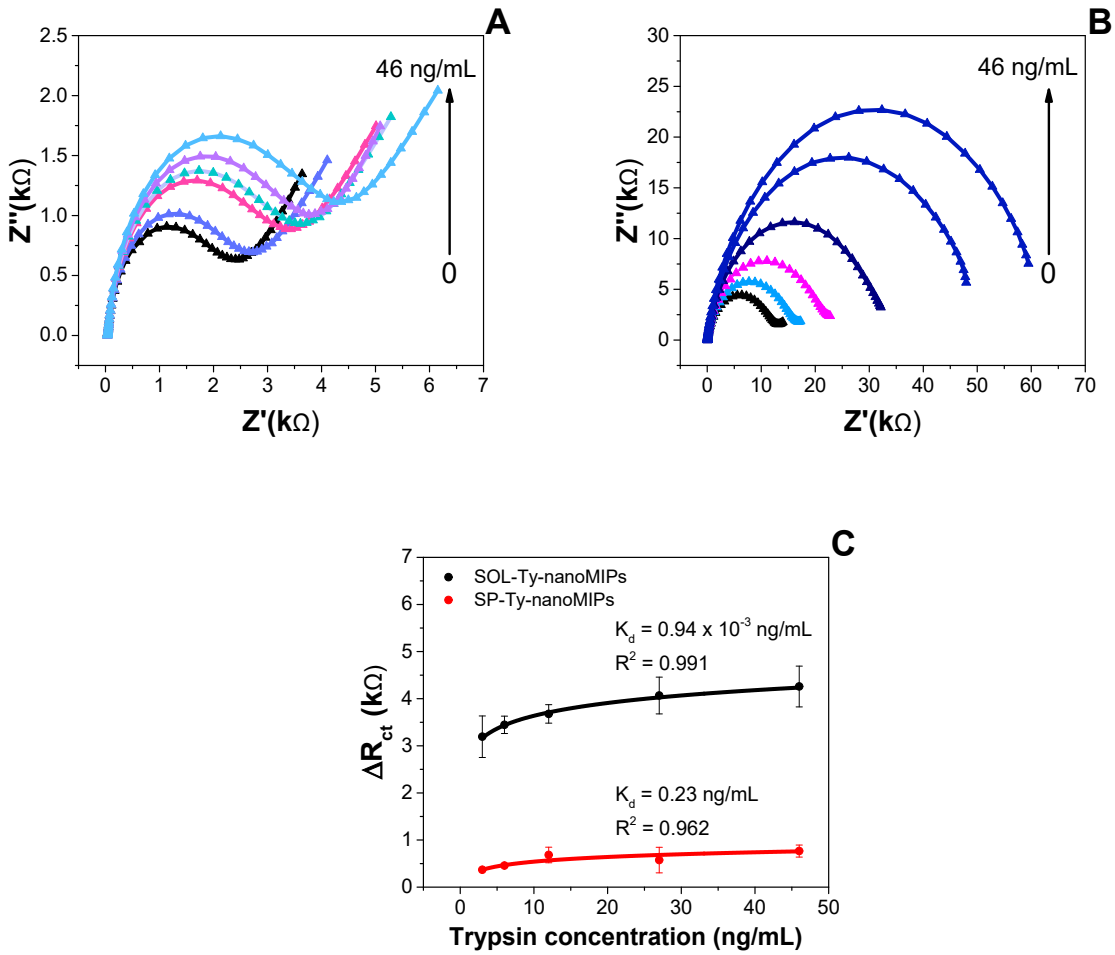

Fig. **S5.** Nyquist plot obtained for (A) SP-Ty-nanoMIPs and (B) SOL-Ty-nanoNIPs sensors after the exposure to increased concentration of Ty (3, 6, 12, 27, 46 ng/mL). EIS spectra were recorded in 10 mM $Fe(CN)_6^{3-/4-}$ + 0.1 M KCl as the electrolyte solution. (C) Calibration plots obtained in the case of SP-Ty-nanoMIPs and SOL-Ty-nanoMIPs sensor. Experimental data were fitted with Temkin isotherm kinetics.

Section 6. Taguchi orthogonal experimental design

Tab. S1. Selected levels for the parameters.

Parameters	Level 1	Level 2	Level 3
CA time X_1, (s),	1500	2100	3000
NPs immobilisation time, X_2 (min),	30	45	50
Loading time, X_3 (min)	5	10	20

Selected levels for parameters are shown in **Tab. S1**. Taguchi orthogonal array (L9) is represented in **Tab. S2**, which reports the experimental results for each trial acquired in the case of SOL-Ty-nanoMIP and nanoNIP, respectively, and the Y response (imprinted factor, IF, at 3 ng/mL of Ty). The S/N ratios (dB) of the IF were collected and evaluated to obtain the optimised conditions.

Tab. S2. Tagutchi orthogonal array matrix, responses of SOL-Ty-nanoMIPs and nanoNIPs sensors, the imprinted factor (IF), and the calculated S/N ratios of the IF

Trial	X1	X2	X3	ΔR_{ct} (Ω)[a]		IF	S/N ratio (dB)
				nanoMIP	nanoNIP		
1	1500	30	5	1113	630	1.77	4.9450
2	1500	45	10	2082	236	8.82	18.9124
3	1500	50	20	1077	144	7.51	17.5093
4	2100	30	10	7854	192	40.94	32.2422
5	2100	45	20	1404	227	6.17	15.8094
6	2100	50	5	2162	310	6.98	16.8759
7	3000	30	20	2510	66.7	37.65	31.5162
8	3000	45	5	9923	6058	1.64	4.2866
9	3000	50	10	1.520	0.102	14.92	23.4780

[a] = R_{ct} (3 ng/mL)-R_{ct} (0)

Table **S3**. Response table for Signal to Noise ratio (criteria: Larger is better)

Level	X_1	X_2	X_3
1	13.78	22.90	8.70
2	21.64	13.00	24.87

3	19.76	19.28	21.61
Delta	7.85	9.89	16.17
Rank	3	2	1

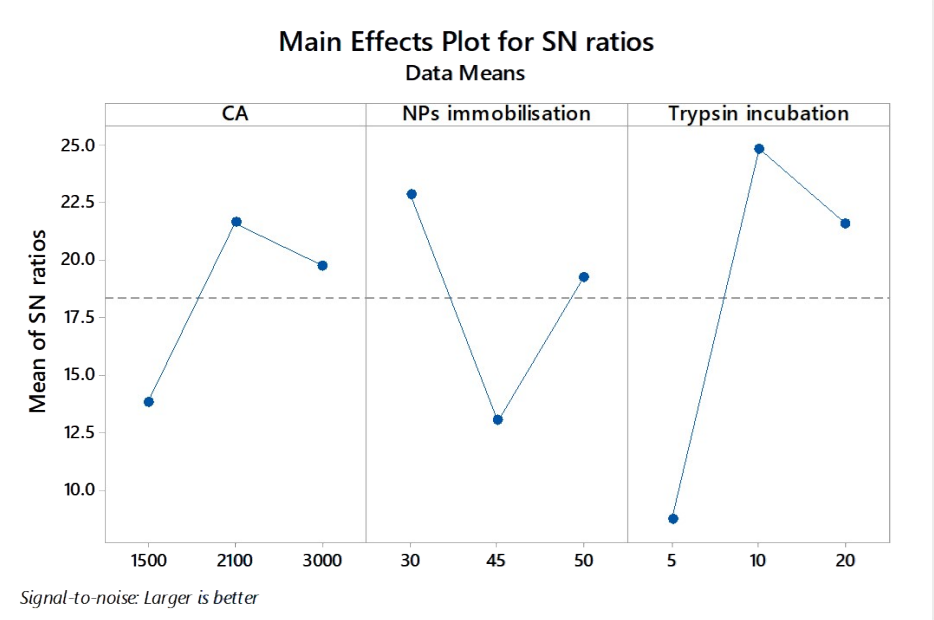

Fig. **S6**. Main effects plot for S/N ratios

Section 7. Analytical assessments on bare SPAuE and TA-SAM/SPAuE

EIS measurements were carried out for bare SPAuE and TA-SAM/SPAuE, respectively, to compare their analytical results with that of SOL-Ty-nanoMIPs/nanoNIPs sensors. Both electrode surfaces were allowed to interact with 100 µL of Ty solution at increased concentration (from 0 to 100 ng/mL) and EIS were recorded. The EIS measurements were carried out in the presence of PBS (0.05 M, pH = 6) containing 10 mM $Fe(CN)_6^{3-/4-}$ as the electrochemical redox probe, in the frequency range from 100 KHz to 0.1 Hz, E_{dc} = + 0.2 V (vs Ag reference), E_{ac} = 0.01 V. As shown in Fig. **S7A**, the bare SPAuE did not respond to the analyte, confirming the analytical observations on Ty-nanoMIPs sensor, which were directly correlated with the affinity's properties of the immobilised receptors. At the same time, EIS spectra for the TA-SAM/SPAuE (Fig. **S7B**) were randomly distributed in the tested range of trypsin concentrations, revealing a not sensitive analytical response.

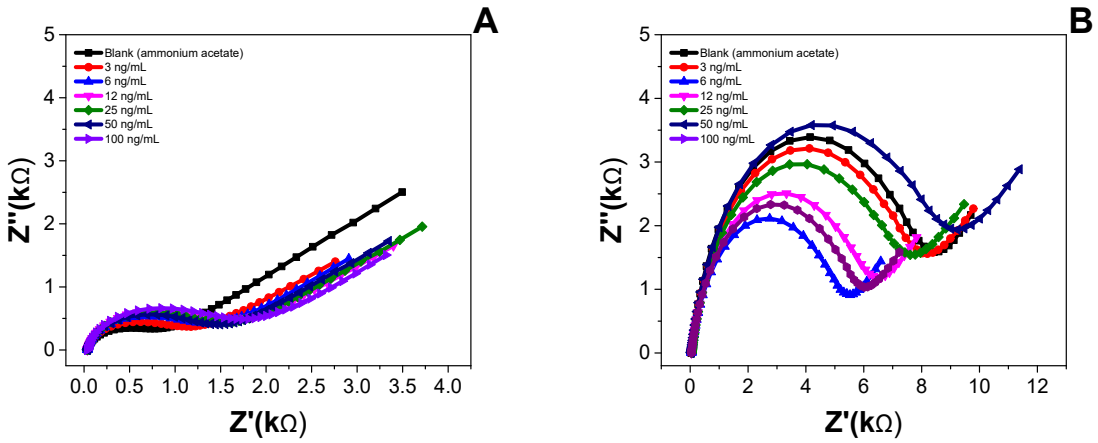

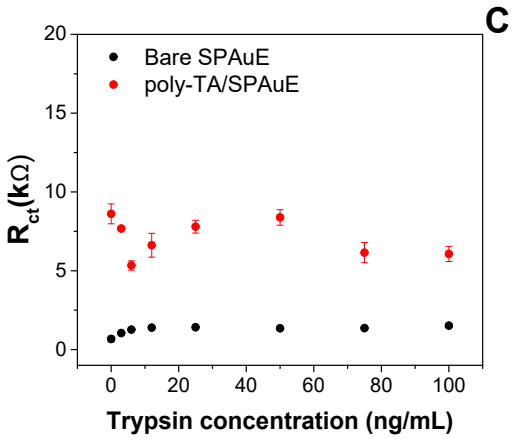

Fig. **S7**. EIS spectra acquired for (A) bare SPAuE, and (B) TA-SAM/SPAuE after the incubation of trypsin between the concentration of 0 (blank, ammonium acetate buffer pH 6) and 100 ng/mL.

The comparison of R_{ct} acquired in the case of bare SPAuE, TA-SAM/SPAuE are shown in **Fig S7C**.

Section 8. Cross-reactivity of SOL-Ty-nanoMIPs sensor

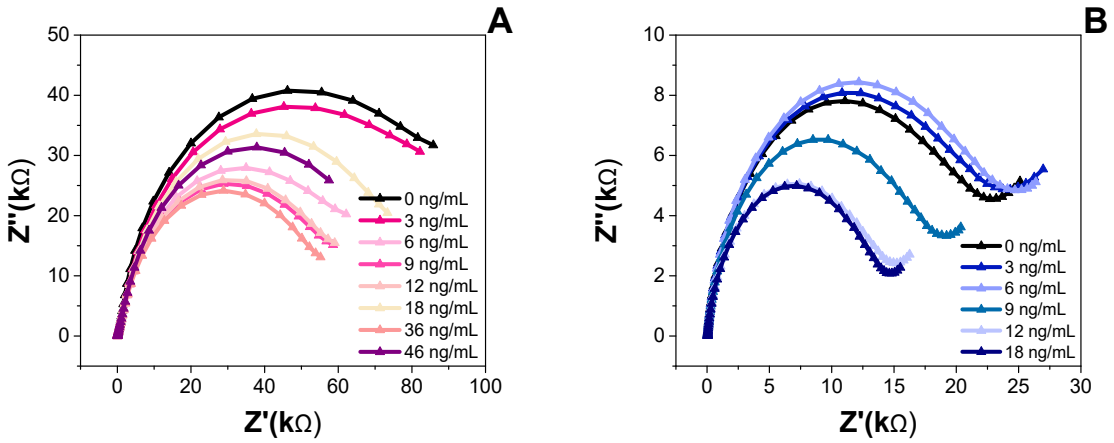

Fig. S**8**. EIS spectra for SOL-Ty-nanoMIPs sensor acquired for (A) pepsin, and (B) mucin at different increased concentration (3, 6, 9, 12, 18, 36, 46 ng/mL) dissolved in ammonium acetate buffer pH 6.